Adaptive PID Control with BP Neural Network Self-Tuning in Exhaust Temperature of Micro Gas Turbine

Jiangjiang Wang, Chunfa Zhang and Youyin Jing
School of Energy and Power Engineering, North China Electric Power University,
Baoding, Hebei Province, 071003 China
Jiangjiang3330@sina.com

Abstract- **Mathematical model of exhaust temperature control in micro gas turbine is introduced. To obtain better performance, a self-adaptive PID control is applied to the exhaust temperature control. The parameters of PID control are tuned by back propagation (BP) neural networks. In the tuning process, the plant's predictive output is used to modify the weights of neural networks. The plant's output is also predicted by BP neural networks and it is nonlinear prediction which improves the predictive accuracy. The effectiveness and efficiency of the proposed control strategy is demonstrated by applying it to the exhaust temperature control. The simulations show that the dynamic responses of the exhaust control system can be effectively improved and the anti-disturbance of the proposed controller is better than that of the PID controller.**

Index Terms – **Back propagation neural network, PID control, self-tuning, exhaust temperature control, micro gas turbine.**

I. INTRODUCTION

In recent years, a growing awareness for the environmental impact of energy consumption and power generation is noticed. Forced by the Kyoto agreement, many countries raise their efforts to cut greenhouse gas emissions. As a result, some countries have enacted some documentaries to reduce greenhouse gas emissions. The China government's goal is to reduce 95 million tons of greenhouse gas emissions by 2010. As cogeneration is a technique to produce heat and power in such a way that less primary energy is needed, it will, in most cases, provide a reduction of greenhouse gas emissions. Therefore, now-a-day cogeneration gains more and more interest [1], resulting in new governmental regulations and a renewed research interest into the potential of micro turbines with new technologies [2, 3].

Micro-turbines have generally evolved from automotive or aerospace small turbine applications, or from efforts to make industrial turbines smaller, and tend to fall in the 5 to 500 kW size range [4]. They are an important part of the evolving distributed power generation picture, which includes stand alone generation, combined cycle applications with fuel cells and combined heat and power applications. The benefits of combining the thermal and electrical outputs of a generating system are widely recognized. Micro-turbines offer a number of potential advantages compared to other technologies for small-scale power generation [5]. For example, compact size and low-weight per unit power leading to reduced civil engineering costs, a small number of moving parts, lower noise, multi-fuel capabilities as well as opportunities for lower emissions (in the Combined Heat Power (CHP) context). In addition, gas turbines enjoy certain merits relative to diesel engines in the context of micro-power generation. They have high-grade waste heat, low maintenance cost, low vibration level and short delivery time. Extracting the exhaust energy that would otherwise be wasted increases the total system efficiency far beyond that of fossil-fuelled utility power plants. This implies less greenhouse gas emissions than using conventional energy conversion technologies. Since micro turbines are already extremely clean burning, other exhaust emissions are reduced as well as in [6].

The micro gas turbine control system is vital to the performance and the energy saving. Some researchers have studied the control of gas turbine [7-15]. In past research, most researchers have paid attention to the speed control. Especially, the intelligent control, fuzzy control, network control, etc, has been applied to the speed control of micro gas turbine [12-14]. However, the exhaust temperature control usually adopts the simple PI control [7-15]. The intelligent control algorithm applied to exhaust temperature is few. Pan Lei designed a neural network robustness controller to the exhaust temperature control [15].

In this paper, micro gas turbine, used in CHP system, requires good mobile tracking performance according to the heat recovery system. So we have made further design of self-adaptive PID controller with back propagation (BP) neural network self-tuning for exhaust temperature control. The BP neural network has applied to many industrial fields [16-19]. Here the self-adaptive BP neural network PID control algorithm is applied to the exhaust temperature control. The improved PID control is simulated and analyzed.

II. MATHEMATICAL MODEL OF EXHAUST TEMPERATURE CONTROL

A thorough introduction to gas turbine theory is provided in the book of Cohen et al. [20]. There also exists a large

978-1-4244-1718-6/08/$25.00 ©2008 IEEE

literature on the modeling of gas turbines. Model complexity varies according to the intended application. Detailed first principles modeling based upon fundamental mass, momentum and energy balances is reported by Fawke et al. [21] and Shobeiri [22]. These models describe the spatially distributed nature of the gas flow dynamics by dividing the gas turbine into a number of sections. Throughout each section, the thermodynamic state is assumed to be constant with respect to location, but varying with respect to time. Mathematically, the full partial differential equations model description is reduced to a set of ordinary differential equations, which facilitate easier application within a computer simulation program.

Instead of applying the fundamental conservation equations, as described above, another modeling approach is to characterize the gas turbine performance by utilizing real steady state engine performance data, as in [23]. It is assumed that the transient thermodynamic and flow processes are characterized by a continuous progression along the steady state performance curves. This is known as the quasi-static assumption. The dynamics of the gas turbine, e.g. combustion delay, motor inertia, fuel pump lag etc., are then represented as lumped quantities, separate from the steady state performance curves. Very simple models result if it is further assumed that the gas turbine is operated at all times close to rated speed [24].

The single shaft micro gas turbine is shown in Fig.1. In the CHP system, there are compressor, combustor, turbine, generator and the heat recovery system, etc. The micro gas turbine operates as follows:

Air at atmospheric pressure enters the gas turbine at the compressor inlet. After the compression of air to achieve the most favorable conditions for combustion, fuel gas (natural gas) is mixed with the air in the combustor, combustion takes place and the hot exhaust gases are expanded through the turbine to produce mechanical power, which is used to generate electricity. The exhaust is sent to the heat recovery system or boiler, etc.

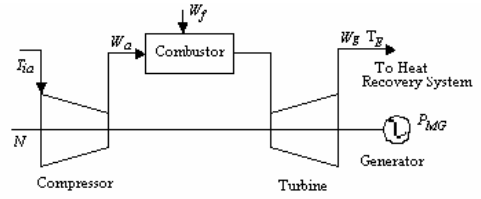

Fig.1 Micro Gas Turbine Structure

The control systems of micro gas turbine include mainly the speed and accelerated speed control, air and fuel control, and exhaust temperature control.

The aim of temperature control system is to limit the gas turbine inlet temperature to avoid too high inlet temperature to damage the turbine lamina. Due to too high temperature, it is difficult to measure. Additionally the exhaust temperature can reflect the inlet temperature. When the inlet temperature rises, the exhaust temperature will also rise. The exhaust temperature will decrease with the decrease of inlet temperature. So the temperature control system of micro gas turbine does not directly control the gas turbine inlet temperature while it directly regulates exhaust temperature to maintain the inlet temperature. Fig.2 shows the control scheme for exhaust temperature TE. C is the controller and the other parameters is as same as [10, 11].

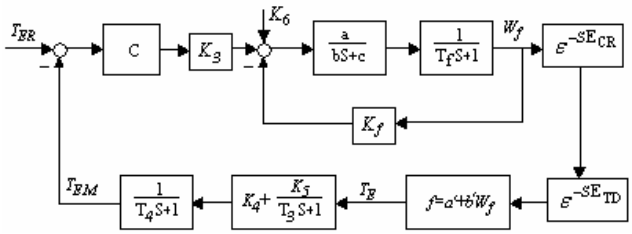

Fig.2 Exhaust Temperature Control

The exhaust temperature reference T_{ER} is fed to the exhaust temperature control. The measured exhaust temperature T_{EM} is different to the actual exhaust temperature T_E due to the radiation shield and thermocouple lags, which is shown in Fig.2.

The measured exhaust temperature T_{EM} is compared with the limit value T_{ER} and the error acts on the temperature controller. Normally T_{EM} is less than T_{ER} causing the temperature controller to be at the MAX limit (about 1.1 per unit) as [10].

The output of temperature controller will regulate the fuel flow into the combustor so that the exhaust temperature is controlled. The fuel system is implement part and is shown in Fig.2.

The fuel supply system consists in two series-wound valves. The first valve is and regulates the gas's pressure that bases on the speed. The second valve is fuel control valve and regulates the fuel flow. The transfer functions are respectively:

$$G(S) = \frac{a}{bs + c} \tag{1}$$

$$G(S) = \frac{1}{t_f s + 1} \tag{2}$$

The fuel signal will regulate and change the exhaust temperature through the combustor time delay E_{CR}, and the turbine and exhaust system transport delay E_{TD}.

The exhaust temperature generally relates to the speed, N, fuel, W_f, inlet vane, v, ambient temperature, T_{ia}, and can be shown as

$$T_E = f(N, W_f, v, T_{ia}) \tag{3}$$

Here the function is simplified as [15] and is expressed to:

$$T_E = a' + b' W_f \tag{4}$$

III. Adaptive PID controller

The controller in Fig. 2 adopts the adaptive PID control, whose parameters are tuned adaptively through BP neural network. The control system is shown in Fig.3, where BP NN C is to tune the PID controller parameters and BP NN P is to predict the plant's output.

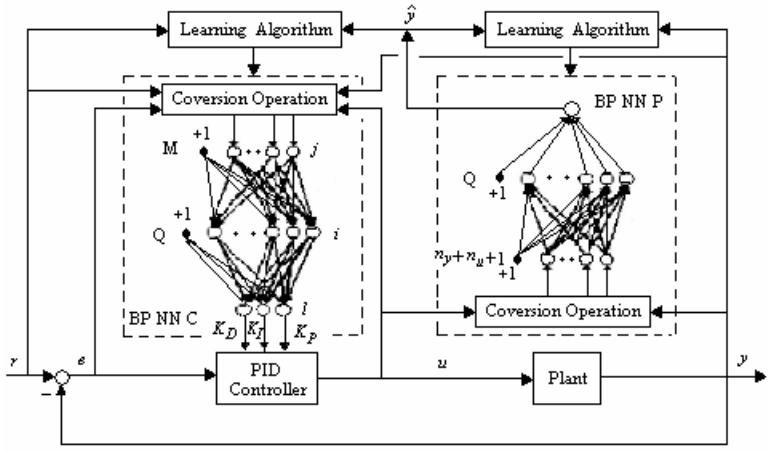

Fig 3 Adaptive PID control system with BP neural network self-tuning

A Neural Network PID Controller

The control system with neural network PID controller is constructed as in Fig.3. The discrete PID controller could be written in a discrete form:

$$u(k) = u(k-1) + K_P[\frac{T_0}{T_i}e(k) + \Delta e(k) + \frac{T_d}{T_0}\Delta^2 e(k)]$$
$$= u(k-1) + K_P\Delta e(k) + K_I e(k) + K_D\Delta^2 e(k) \quad (5)$$

where:

$$K_I = K_P T_0 / T_i, K_D = K_P T_d / T_0$$
$$e(k) = r(k) - y(k)$$
$$\Delta e(k) = e(k) - e(k-1)$$
$$\Delta^2 e(k) = e(k) - 2e(k-1) + e(k-2)$$

where K_P, K_I, K_D are respectively the proportional, integral and derivative gains of the PID controller which should be tuned and optimized. T_i is the integration time, T_d is the derivative time of the PID controller, and T_0 is the sampling time.

Equation (5) can be recomposed as follows:

$$u(k) = f(u(k-1), K_P, K_I, K_D, e(k), e(k-1), e(k-2)). \quad (6)$$

where $f[\cdot]$ is a nonlinear function that is concerned with K_P, K_I and K_D. The best control rule can be discovered by the training and learning of BP neural network.

The BP NN C in Fig.3 can be used to adjust the gains of PID controller adaptively by using the BP method with measurement data of $u(k)$, $y(k)$, and $r(k)$. The BP network is a multilayered network which consists of an input layer, an output layer, and several hidden layers of nonlinear processing elements. In this paper, the three layers BP NN is used as Fig. 3, which has M input neurons, Q hidden neurons and three output neurons. The input neurons can be the state of system, for example the input or output of different times, which should be normalized as [25] if the network needs. The output of BP NN C, respectively, is the three tuned parameters of PID controller. Because the three parameters K_P, K_I and K_D can't be negative, the activation function of output layer's neurons is Sigmoid function that is not negative and the activation function of hidden layer's neurons is Sigmoid function that is symmetry of positive and negative.

In Fig. 3 the output of input layer's neurons of BP neural network can be expressed as follows:

$$o_j^{(1)} = x_{k-j}, j = 0,1,...,M-1,$$
$$o_M^{(1)} \equiv 1. \quad (7)$$

where $o_j^{(1)}$ is the output of *j-th* neuron in input layer, the number of input layer's neurons M lies on the complex degree of the control system. In the equations, the superscript symbols (1), (2) and (3) are, respectively, the input layer, hidden layer and output layer.

The input and output of hidden layer can be expressed:

$$net_i^{(2)}(k) = \sum_{j=0}^{M} w_{ij}^{(2)} o_j^{(1)}(k),$$
$$o_i^{(2)}(k) = f[net_i^{(2)}(k)], i = 0,1,...,Q-1, \quad (8)$$
$$o_Q^{(2)}(k) \equiv 1.$$

where $net_i^{(2)}$ is the input of *i-th* neuron in hidden layer, $w_{ij}^{(2)}$ is the weights of hidden layer, $w_{iM}^{(2)}$ is the valve value; $f[\cdot]$ is the activation function that is $f[\cdot] = \tanh(x)$

The input and output of output layer can be expressed:

$$net_l^{(3)}(k) = \sum_{i=0}^{Q} w_{li}^{(3)} o_i^{(2)}(k),$$
$$o_l^{(3)}(k) = g[net_l^{(3)}(k)], l = 0,1,2,$$
$$K_P(k) = o_0^{(3)}(k), \quad (9)$$
$$K_I(k) = o_1^{(3)}(k),$$
$$K_D(k) = o_2^{(3)}(k).$$

where $w_{li}^{(3)}$ is the weights of output layer, $w_{lQ}^{(3)}$ is the valve value, $w_{lQ}^{(3)} = \theta_l$ $g[\cdot]$ is the activation function and $g[\cdot] = [1 + \tanh(x)]/2$.

By using the BP algorithm based on gradient method, to minimize the performance index function J which can be expressed as following:

$$J = \frac{1}{2}[r(k+1) - y(k+1)]^2 = \frac{1}{2}e^2(k+1). \quad (10)$$

where J is to modify the weights by the fastest descend mean, which is searched and tuned toward the negative gradient and added on a inertia coefficient to make faster constringency, and:

$$\Delta w_{li}^{(3)}(k+1) = -m\frac{\partial J}{\partial w_{li}^{(3)}} + a\Delta w_{li}^{(3)}(k). \quad (11)$$

where m stands for the velocity of learning, a is smoothing coefficient.

$$\frac{\partial J}{\partial \omega_{li}^{(3)}} = \frac{\partial J}{\partial y(k+1)}\frac{\partial y(k+1)}{\partial u(k)}\frac{\partial u(k)}{\partial o_l^{(3)}(k)}\frac{\partial o_l^{(3)}(k)}{\partial net_l^{(3)}(k)}\frac{\partial net_l^{(3)}(k)}{\partial \omega_{li}^{(3)}}. \quad (12)$$

In (12) $\frac{\partial y(k+1)}{\partial u(k)}$ is not known so that it can be replaced by $\frac{\partial \hat{y}(k+1)}{\partial u(k)}$, which can be calculated in the nonlinear model or least-squares method. Here $\frac{\partial \hat{y}(k+1)}{\partial u(k)}$ is predicted in neural network.

In (5) the difference of $u(k)$ to K_P, K_I, K_D can be expressed as following:

$$\begin{aligned}
&\frac{\partial u(k)}{\partial o_0^{(3)}(k)} = e(k) - e(k-1),\\
&\frac{\partial u(k)}{\partial o_1^{(3)}(k)} = e(k),\\
&\frac{\partial u(k)}{\partial o_2^{(3)}(k)} = e(k) - 2e(k-1) + e(k-2).
\end{aligned} \quad (13)$$

So, the weights of output layer in BP neural network are updated as following:

$$\begin{aligned}
&\Delta w_{li}^{(3)}(k+1) = m\delta_l^{(3)}o_i^{(2)}(k) + a\Delta\omega_{li}^{(3)}(k),\\
&\delta_l^{(3)} = e(k+1)\cdot\frac{\partial \hat{y}(k+1)}{\partial u(k)}\cdot\frac{\partial u(k)}{\partial o_l^{(3)}(k)}g'[net_l^{(3)}(k)],\\
&l = 0,1,2.
\end{aligned} \quad (14)$$

According as the mean like above, the weights of hidden layers are updated as following:

$$\begin{aligned}
&\Delta w_{ij}^{(3)}(k+1) = m\delta_i^{(2)}o_j^{(1)}(k) + a\Delta\omega_{ij}^{(2)}(k),\\
&\delta_i^{(2)} = f'[net_i^{(2)}(k)]\sum_{l=0}^{2}\delta_l^{(3)}\omega_{li}^{(3)}(k),\\
&i = 0,1,...,Q-1.
\end{aligned} \quad (15)$$

where

$$\begin{aligned}
&g'[\cdot] = g(x)[1-g(x)],\\
&f'[\cdot] = [1-f^2(x)]/2.
\end{aligned} \quad (16)$$

B Prediction

The controlled object is supposed to a nonlinear system that is single input and single output system as following:

$$\begin{aligned}
y(k) = f[&y(k-1), y(k-2), ..., y(k-n_y),\\
&u(k-1), u(k-2), ..., u(k-n_u)]
\end{aligned} \quad (17)$$

where $y(k)$ and $u(k)$ are the output and input on the k time, n_y and n_u are the order of $\{y\}$ and $\{u\}$, $f[\cdot]$ is the nonlinear function.

To calculate the prediction of $\hat{y}(k+1)$, there is a three layers BP neural network model (BP NN P in Fig.3) as the prediction model which has $n_y + n_u + 1$ input neurons, Q hidden neurons and one output neuron. For the sake of prediction of nonlinear system easily, the activation function of output layer is linear function and the activation function of hidden layer's neurons is still Sigmoid function.

The prediction calculation of BP neural network model: let the input and output of the plant $\{y(k)\}$ and $\{u(k)\}$ be the neural network model's input, and the input layer:

$$\begin{aligned}
&o_j^{(1)}(k) = \begin{cases} y(k-j) & 0 \le j \le n_y - 1 \\ u(k-j+n_y) & n_y \le j \le n_y + n_u - 1 \end{cases}\\
&o_{n_y+n_u}^{(1)}(k) = 1.
\end{aligned} \quad (18)$$

The input and output of hidden layer can be expressed:

$$\begin{aligned}
&net_i^{(2)}(k) = \sum_{j=0}^{n_y+n_u} w_{ij}^{(2)}o_j^{(1)}(k),\\
&o_i^{(2)}(k) = f[net_i^{(2)}(k)],\\
&o_Q^{(2)}(k) \equiv 1,\\
&i = 0,1,...,Q-1.
\end{aligned} \quad (19)$$

where $w_{ij}^{(2)}$ is the weights of hidden layer, $w_{in_y+n_u}^{(2)}$ is the valve value and $\omega_{in_y+n_u}^{(2)} = \theta_i$, $f[\cdot]$ is the activation function and $f[\cdot] = \tanh(x)$.

And the output of output layer can be expressed as following:

$$\hat{y}(k+1) = \sum_{i=0}^{Q} w_i^{(3)}o_i^{(2)}(k). \quad (20)$$

where $w_i^{(3)}$ is the weights of output layer, $w_Q^{(3)}$ is the valve value and $w_Q^{(3)} = \theta_0$, and the output neuron is linear neuron.

The backward learning of BP NN P: use the learning algorithm of BP to modify the weights and valve value and make the target function J_y minimum:

$$J_y = \frac{1}{2}[y(k+1) - \hat{y}(k+1)]^2. \quad (21)$$

and the weights is modified as following:

$$\Delta w_i^{(3)}(k+1) = m[y(k+1) - \hat{y}(k+1)]o_i^{(2)}(k) + \alpha\Delta\omega_i^{(3)}(k),$$
$$\Delta w_{ij}^{(2)}(k+1) = m[y(k+1) - \hat{y}(k+1)] \cdot f'[net_i^{(2)}(k)]w_i^{(3)}(k)o_i^{(3)}(k) + \alpha\Delta\omega_{ij}^{(2)}(k), \quad (22)$$
$$i = 0,1,...,Q,$$
$$j = 0,1,...,n_y + n_u.$$

where m is the velocity of learning, a is smoothing coefficient, and both is in the $(0,1)$

The derivative of activation function can be expressed:

$$f'(x) = [1 - f^2(x)]/2. \quad (23)$$

So $\frac{\partial\hat{y}(k+1)}{\partial u(k)}$ can be expressed as following:

$$\frac{\partial\hat{y}(k+1)}{\partial u(k)} = \sum_{i=0}^{Q}\left(\frac{\partial\hat{y}(k+1)}{\partial o_i^{(2)}(k)} \cdot \frac{\partial o_i^{(2)}(k)}{\partial net_i^{(2)}(k)} \cdot \frac{\partial net_i^{(2)}(k)}{\partial u(k)}\right)$$
$$= \sum_{i=0}^{Q}(\omega_i^{(3)} f[net_i^{(2)}(k)]w_{in_y}^{(2)}(k)). \quad (24)$$

IV. Simulation

Adaptive PID controller with BP neural network self-tuning and traditional PID controller are both simulated to compare. Based on reference [7, 9, 10, 11], the parameters in Fig.2 are shown in Table I.

The parameters of traditional PID controller are optimized and got: K_P=0.229, K_I =0.005, K_D =7.5.

TABLE I
PARAMETERS VALUES

K_3=0.77	K_4=0.8	K_5=0.2	K_6=0.23
K_f=0	a=1	b=0.05	c=1
T_d=2.5	T_3=15	T_f=0.4	
E_{CR}=0.01	E_{TD}=0.1		

The neural network PID in the simulation is 6-8-3, the velocity of learning $\eta = 0.25$, the flatness coefficient $a = 0.01$, and the initial weights is the random number in the extent $[-1.0,1.0]$.

The simulations include the step response and the anti-disturbance response. Firstly the step responses are simulated. When t=0, the desired input is stepped from 0 to 1 and when t=50s, the desired input is stepped from1 to 0.5. The simulation results are shown in Fig.4 and Fig.5. From them it can be seen that the governing time of adaptive PID control is shorter than traditional PID control. Due to the self-tune at the begin, the overshoot of adaptive PID control is greater than traditional PID control, however, there are less overshoot of adaptive PID control than traditional PID control when the second step is input.

The parameters of self-adaptive PID controller are shown in Fig.6. It is seen that the parameters of PID controller are tuned on-line in BP neural network, which is helpful to the control system performance. Due to the tune at the begin, the step response of adaptive PID control has greater overshoot.

Secondly the anti-disturbance responses are simulated. In Fig.2 a' increases 0.5 when t=50s. The anti-disturbance responses of traditional PID control and adaptive PID control are respectively shown in Fig.7 and Fig.8. From the simulation results, it can be found that the overshoot are both equivalent while the governing time of adaptive PID control is shorter than traditional PID control when the disturbance is entered into the system at t=50s. Moreover, there is little surge in the traditional PID control while the curve of adaptive PID control is very stable. Figure 9 shows the parameters of self-adaptive PID controller. When the disturbance the disturbance is entered into the system, the differential gain makes the system's performance better.

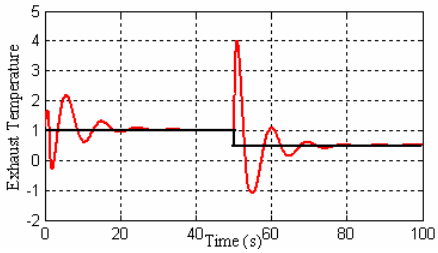

Fig 4 Step response of PID control for exhaust temperature

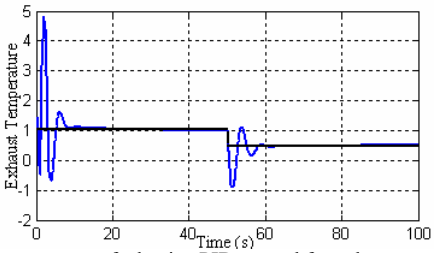

Fig 5 Step response of adaptive PID control for exhaust temperature

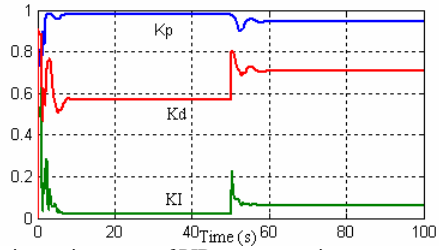

Fig 6 Adaptive tuning curve of PID parameters in step response simulation

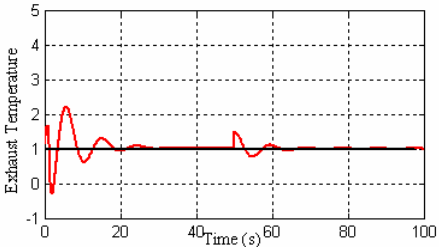

Fig 7 Anti-disturbance response of PID control

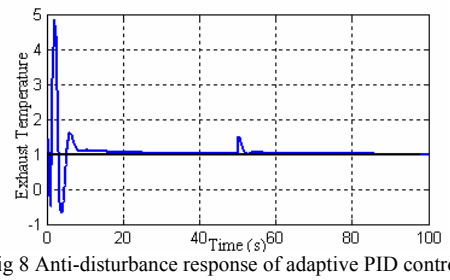

Fig 8 Anti-disturbance response of adaptive PID control

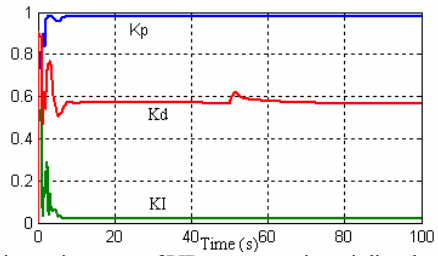

Fig 9 Adaptive tuning curve of PID parameters in anti-disturbance simulation

V. Conclusion

This study has demonstrated that the adaptive PID control system with BP neural network self-tuning can achieve favorable tracking performance and anti-disturbance for the exhaust temperature control in the micro gas turbine.

The BP neural network is used to tune the PID parameters and to predict the plant output. The traditional PID controller has self-adaptive capability through the BP neural network learning and training. Therefore, the adaptive PID controller in this paper has excellent anti-disturbance and adaptively.

From the simulation results, it can be seen that the overshoot of adaptive PID controller in this paper is greater than traditional PID controller while the governing time of adaptive PID controller is shooter, which is helpful to the safety of micro gas turbine.

Acknowledgment

The authors would like to acknowledge the financial and technical support of the Key Laboratory of Condition Monitoring and Control for Power Plant Equipment of Ministry of Education, China, during the course of this research.

References

[1] Conde Lazaro E, Ramos Millan A, Reina Peral P, "Analysis of Cogeneration in the Present Energy Framework", *Fuel Process Technology*, Vol.87, pp.163-168, 2006.

[2] Michel DP, Peter DH, David M, "Micro-CHP Systems for Residential Applications," *Energy Conversion and Management*, Vol.47, pp.3435-3446, 2006.

[3] E.Cardona, A. Piacentino, F. Marchese, "Performance Evaluation of CHP Hybrid Seawater Desalination Plants," *Desalination*, Vol.205, pp.1-14, 2007.

[4] Francisco Jurado, Antonio Cano and Jose Carpio, "Biomass based micro-turbine plant distribution network stability," *Energy Conversion and Management*, vol. 45, pp 2713-2727, 2004.

[5] P.A. Pilavachi, "Power generation with gas turbine systems and combined heat and power," *Applied Thermal Engineering*. vol. 20, pp 1421-1429, 2000.

[6] P.Li, P. Degobert, B. Francois and B. Rbyns, "Modeling and control of a gas micro turbine generator by using a causal ordering graph," Proceedings of IMACS Multi-conference on Computational Engineering in Systems Applications, pp.271-277, Beijing, China, October 4-6, 2006.

[7] Wei Siliang, Liu Shangming and Ni Weidou, "Simulation of gas turbine with droop control system under Matlab/Simulink," *Power Engineering*, vol. 21, no.6, pp 1555-1559, 2001.

[8] Zhao Jingfeng, Ye Chun and Qin Chunshen, "Study on integrate modeling of gas turbine and its control system," *East China Electric Power*, vol. 33, no.4, pp 13-16, 2005.

[9] Wei Siliang, Liu Shangming and Ni Weidou, "Dynamic model research of a single-shaft gas turbine in mechanical drive applications," *Journal of Engineering for Thermal Energy and Power*, vol. 16, no.3, pp 303-307, 2001.

[10] Working Group on Prime Mover and Energy Supply Models for System Dynamic Performance Studies, "Dynamic models for combined cycle plants in power system studies," *IEEE Transactions on Power Systems*. vol. 9, no.3, pp 1698-1708, 1994.

[11] L. N. Hannett and Afzal Khan, "Combustion turbine dynamic model validation from tests," *IEEE Transactions on Power Systems*, vol. 8, no.1, pp 152-158, February 1993.

[12] Yue Junhong, Liu Jizhen, Tan Wen and Liu Xiangjie, "Fuzzy PID controller for micro-turbine rotate speed," *Gas Turbine Technology*, vol. 19, no.4, pp 43-46, 2006.

[13] Wei Deng and Huanguang Zhang, "Fuzzy neural networks adaptive control of micro gas turbine with prediction model," Proceeding of the 2006 IEEE International Conference on Networking, Sensing and Control, pp 1053-1058, 23-25 April 2006.

[14] Xu Lixin, Qiang Wenyi and Zhou Yan, "Decoupling control in single shaft gas turbine plant based on fuzzy neural network," *Turbine Technology*, vol. 46, no.6, pp 421-424, 2004.

[15] Pan Lei, Yang Yuwen and Lin Zhongda, "Neural network robustness control and it's emulation in the exhaust temperature control gas turbine," *Power Engineering*, vol. 21, no.6, pp 1542-1547, 2001.

[16] Junbin Liang and Jianmin Xu, "Intelligent control and tracking identification of magnetorheological damper based on improved BP neural networks," Proceeding of the Sixth World Congress on Intelligent Control and Automation, Dalian, China, 2006.

[17] Li Guozhu, Kaishan Song, and Shuwen Niu, "Soybean LAI estimation with in-situ collected hyper spectral data based on BP-neural networks," Proceeding of the 3rd International Conference on Recent Advances in Space Technologies, pp 331-336, June 14-16, 2007.

[18] Wang Wen, Fei Shumin, Zheng Bo, Wu Chengyun and Wen Yaoqi, "Application of data mining technology based on BP neural network in yarn qualities forecast," Proceeding of the 2006 Chinese Control Conference, pp 1926-1929, Harbin, China, August 7-11, 2006.

[19] Wang Binghe, Guo Hongxia, Zheng Siyi and Yang Xilin, "TCM pulse-condition classification method based on BP neural network," Proceeding of the First International Conference on Bioinformatics and Biomedical Engineering, pp 629-632, July 6-8, 2007.

[20] Cohen H, Rogers GFC, Saravanamuttoo HIH. *Gas turbine theory*. 4th ed. England: Longman; 1998.

[21] Fawke AJ, Saravanamuttoo HIH, Holmes M, "Experimental verification of a digital computer simulation method for predicting gas turbine dynamic behaviour," *Inst Mech Engrs Proc*, vol. 186, no.27, pp 323-329, 1972.

[22] Shobeiri T. *Digital computer simulation of the dynamic operating behaviour of gas turbines*. Brown Boveri Rev 1987;(3).

[23] Hung WW, "Dynamic simulation of gas-turbine generating unit," *IEE Proceeding of Control*, vol. 138, no.4, pp 342-350, 1991.

[24] Rowen WJ, "Simplified mathematical representations of heavy duty gas turbines," *ASME Journal of Engineering Power*, vol. 5, no.4, pp 865-869, 1983.

[25] J. Yi and Y. Hou, *Intelligent Control*, Beijing: Beijing University of Technology Press, 1999.